



Published in final edited form as:

Mol Cancer Ther. 2015 October ; 14(10): 2198–2205. doi:10.1158/1535-7163.MCT-15-0401.

Intrapulmonary Delivery of CpG Microparticles Eliminates Lung Tumors

Takashi Sato^{1,3}, Takeshi Shimosato², Atsuhisa Ueda³, Yoshiaki Ishigatsubo³, and Dennis M Klinman¹

¹Cancer and Inflammation Program, National Cancer Institute, Frederick, MD 21702

²Graduate School of Agriculture, Shinshu University, Nagano 399-4598, Japan

³Graduate School of Internal Medicine and Clinical Immunology, Yokohama City University, Yokohama 236-0004, Japan

Abstract

CpG oligonucleotides (ODN) stimulate the innate immune system by triggering cells that express TLR9. The resulting response promotes tumor regression, an effect optimized by delivery of CpG ODN to the tumor site. This work examines the effect of instilling CpG ODN adsorbed onto polyketal microparticles (CpG-MP) into the lungs of mice with non-small cell lung cancer. Intrapulmonary delivery of CpG-MP improved ODN uptake and retention at the tumor site thereby inducing a stronger Th1 response than systemically administered or unadsorbed CpG ODN. CpG-MP reversed the immunosuppression that characterized the tumor micro-environment by i) decreasing the number of immunosuppressive Tregs and M2 macrophages while ii) increasing the number of tumoricidal CD8⁺ T cells and M1 macrophages. These effects promoted tumor regression and culminated in 82% permanent survival of mice with otherwise fatal Lewis Lung cancer.

Keywords

immune stimulation; innate immunity; TLR9; cancer; microparticles

Introduction

Lung cancer is the leading cause of cancer-related death in the United States with non-small cell lung cancer (NSCLC) accounting for 85% of these tumors (1). Despite recent advances in multi-modal targeted and tailored therapies, the 5-year survival rate for NSCLC remains poor ($\approx 15\%$). Accumulating evidence suggests that controlling the primary tumor can enhance survival even in patients with advanced/metastatic disease (2;3)(NCT01242800 <http://clinicaltrials.gov/show/NCT01242800>). Since most lung tumors are poorly

Corresponding Author: Dr. Dennis M Klinman, National Cancer Institute, Building 567, Room 205, Frederick, MD 21702, 301 228 4265, klinmand@mail.nih.gov.

Conflict of interest statement: Members of Dr. Klinman's lab have patents related to the use of CpG oligonucleotides. All rights to such patents have been assigned to the Federal Government.

immunogenic and resistant to immune surveillance, novel approaches to activating the pulmonary immune system may be key to promoting tumor regression (4;5).

One strategy to trigger the innate immune system involves activating cells that express Toll-like receptors (TLRs). Our group and others find that stimulating cells bearing TLR9 using synthetic oligonucleotides expressing unmethylated CpG motifs (CpG ODN) generates substantial anti-tumor activity (reviewed in (6;7)). For example, treatment with CpG ODN in combination with chemotherapy significantly prolonged survival in a murine Lewis lung cancer model (8). Based on considerable preclinical data, clinical trials assessing the safety and efficacy of systemically administered CpG ODN were conducted in patients with advanced NSCLC (9;10). While favorable results were observed in phase 2 studies, no survival benefit was observed in a phase 3 trial of CpG ODN (11;12). Yet the objective response rate of patients who received CpG ODN exceeded that of patients receiving chemotherapy alone in those studies (28 – 30% vs 19 – 23%). A possible explanation for these inconsistent clinical findings could be that systemically administered CpG ODN either did not reach or did not persist in many pulmonary tumors. In this context, recent studies demonstrate that intra-tumoral delivery optimizes the therapeutic utility of CpG ODN. While systemic administration promotes the development of cancer-specific CTL, the lytic activity of such cells is inhibited by immunosuppressive cells in the tumor microenvironment. Local (but not systemic) delivery of CpG ODN has been shown to reverse this local immunosuppression (13).

Given the limited success of systemic CpG therapy for the treatment of lung cancer, we examined whether intrapulmonary delivery might be more efficacious. Previous studies demonstrated that immunomodulatory ODN could be safely delivered to mice via intra-tracheal instillation (mimicking inhalational therapy in humans). To improve tumor targeting and pulmonary retention, we adsorbed the CpG ODN onto polyketal microparticles previously shown to be safe and efficient for inhalational administration of therapeutic agents (14–17). Polyketal nanoparticles are biodegradable and can be formulated into microparticles optimized for delivery to distal bronchi (18;19). When CpG-MP were delivered intra-tracheally to mice with Lewis lung cancer (a model of human NSCLC), they accumulated and persisted in the tumor microenvironment. This treatment promoted intratumoral immunity while reducing immunosuppression, culminating in a significant reduction in tumor burden and significantly improved survival.

Materials and methods

Preparation of polyketal nanoparticles

A poly-(1,4-phenyleneacetone dimethylene ketal) matrix of nanoparticles was synthesized by Celagix Res Ltd. (Yokohama, Japan). Polyvinylalcohol (PVA, Sigma, St. Louis, MO) was used as the dispersing agent. Polyketal nanoparticles were produced via an acetal exchange reaction as previously described (18;20). Briefly, 2.5 gm of polyketal nanoparticles were synthesized by dissolving 10 gm of 1,4-benzenedimethanol (36 mmol) and 8.6 gm of 1,5-pentanediol (8.67 mmol) in ethyl acetate and adding this to 100 ml of methylbenzene. Recrystallized *p*-toluenesulfonic acid (520 mg, 2.93 mmol) in 1.0 ml of ethyl acetate was then added followed by 2,2-dimethylpropane (9 ml, 37 mmol) to initiate

the reaction. Additional 2,2-dimethylpropane (9 ml, 37 mmol) and methylbenzene was added to the reaction every 30 min for 2 h. After 12 h, the polymer was isolated by precipitation in ice cold hexane (-20°C) followed by vacuum filtration.

Preparation of CpG ODN adsorbed polyketal NP

The phosphorothioate ODN used in this study were CpG 1555 (GCTAGACGTTAGCGT) and control ODN 1612 (GCTAGAGCTTAGCGT). These were synthesized by IDT Technologies (Coralville, IA). ODN were adsorbed onto polyketal nanoparticles using the water-in-oil-in-water double emulsion solvent evaporation method (21). ODN dissolved in water was added to DOTAP solution (Avanti, Alabaster, AL) at a 1:1 (w/w) ratio with stirring. The ODN/DOTAP complexes were added to a 0.5% w/v PVA solution in 10 mM sodium bicarbonate and then mixed with a solution of polyketal (500 mg) dissolved in 5 ml of dichloromethane. The mixture was emulsified by sonication (Sonifier 250, Branson, USA, Duty cycle 80%, output 5) for 3 min. The resulting emulsion was added to 125 ml of a 1% PVA solution and agitated with stirring at 500 rpm for 6 h to remove dichloromethane. The ODN-loaded polyketal nanoparticles were collected by centrifugation at 4,500 rpm for 10 min, washed with 10 mM sodium bicarbonate and then freeze-dried to form microparticles (MP). All materials in this study were endotoxin free as determined by *Limulus* amoebocyte cell lysate assay (Cambrex Bioscience, Walkersville, MD; sensitivity 0.1 U endotoxin/mg).

The release of CpG ODN from CpG-MP dissolved in physiological saline (pH 7.4, 37°C) was examined. Supernatants were collected over time, centrifuged at 4500 rpm for 10 min and loaded onto a 3% agarose gel. Gel electrophoresis was performed at 100 V for 0.5 h and the ODN visualized by SYBR staining (Invitrogen) in comparison to serial dilutions of free ODN. Loading efficiency (%) was calculated by the formula: (maximal release of ODN from CpG-MP)/(weight of ODN used in synthetic process) \times 100%.

Analysis of CpG-MP size

CpG-MP samples were suspended in physiological saline, transferred onto carbon tape, and dried. They were then coated with a 30 nm layer of osmium using an osmium plasma coater (NL-OPC80NS, Nippon Laser & Electronics Laboratory, Japan), and visualized by scanning electron microscopy (JSM-6340F) at an acceleration voltage of 5.0 kV.

CpG-MP samples were also suspended in 70% ethanol, absorbed onto a 400 mesh formvar film-coated grid and then visualized by transmission electron microscopy (JEM-1200EX; JEOL Ltd., Japan) at an acceleration voltage of 80 kV. Digital images were taken with a CCD camera (VELETA, Olympus Soft Imaging Solutions GmbH).

Treatment protocols and tumor cell implantation

C57BL/6, TLR9 KO and Rag1 KO mice were obtained from the National Cancer Institute (Frederick, MD) and studied at 5–6 wk of age. Lewis lung carcinoma (LLC1) cells were obtained from American Type Culture Collection in 2012 (Manassas, VA). All experiments with this cell line were performed within 2 months of thawing the cryopreserved cells which were expanded in RPMI-1640 medium supplemented with 2% fetal bovine serum, penicillin

(100 U/ml), streptomycin (0.1 mg/ml), 2 mM glutamate and 1% NEAA. On the day of inoculation, cultured cells were trypsinized, washed and suspended in 0.9% saline. Their viability exceeded 95%.

Tumor challenge studies were performed by instilling 10^6 LLC cells in 50 μ l of saline via orotracheal intubation to anesthetized mice as previously described (22;23). One week later, free ODN or ODN-MP were administered either systemically (i.p.) or locally (i.t.). Instillation was achieved via orotracheal intubation using a 20 gauge 1" catheter (TERUMO, Somerset, NJ) under anesthesia. 4–6 mice per group were used in each experiment and all results derived by combining data from 2–4 independent experiments. All animals were monitored 3X/wk and moribund mice euthanized as per Institutional Animal Care and Use Committee protocol.

Tissue collection and evaluation of tumor development

Bronchoalveolar lavage (BAL) fluid was obtained by tracheal cannulation of anesthetized mice. Cell differentials were performed on cytocentrifuged BAL preparations after fixation and staining with Diff-Quick (Dade Behring, Newark, DE). IL-12 levels in BAL and serum were determined by ELISA. Lungs were inflated and fixed by instilling 1 ml of 10% neutral-buffered formalin or periodate lysine paraformaldehyde (PLP) fixative (Wako Chemicals USA, Inc. Richmond, VA) at 20 cm H₂O. Fixed tissue was embedded in paraffin, sectioned, and stained with hematoxylin and eosin for histopathological assessment. Tumor area was evaluated in mid-line sections and quantified using Image J software ver.1.48 (National Institute of Health, Bethesda, MD).

***In vitro* cell proliferation assay**

Single spleen cell suspensions were prepared. 5×10^4 cells/well were cultured in 96-well flat bottomed microtiter plates in complete RPMI 1640 medium supplemented with 10% fetal calf serum, 100 U/mL penicillin, 100 mg/mL streptomycin, 25 nmol/L HEPES, 1 mmol/L sodium pyruvate, NEAA, and 0.0035% 2-ME. The cells were stimulated with free ODN, ODN-MP, or R837 (TLR7 agonist) for 72 hr. Cell proliferation was assessed using the CCK-8 assay as per manufacturer's recommendation (Dojindo molecular technologies, Inc. Rockville, MD).

Immunohistochemistry and immunofluorescent analysis

Tissue sections were deparaffinized with xylene and rehydrated with graded ethanol. Endogenous peroxidase activity was blocked by incubation with 0.3% H₂O₂ in methanol for 30 min followed by Protein Block (Dako, Carpinteria, CA). They were then stained with the following primary antibodies: rat anti-Foxp3 (eBioscience, San Diego, CA; clone FKJ-16s, dilution 1:200), rat anti-F4/80 (AbD serotec, Raleigh, NC; clone CI:A3-1, dilution 1:300), rabbit anti-CD3 (LSBio, Seattle, WA; clone EPR4517, dilution 1:100), rat anti-CD8 (LSBio; clone CT-CD8a, dilution 1:100), hamster anti-CD11c (Abcam, Cambridge, MA; clone N418, dilution 1:100), rat anti-CD45R/B220 (BD Pharmingen, San Jose, CA; clone RA3-6B2, dilution 1:20), rabbit anti-CD205 (Abcam; clone EPR5233, dilution 1:500), or rabbit anti-CD206 (Abcam; dilution 1:2000). Isotype matched negative controls were included to insure specificity.

For immunohistochemistry, stained sections were incubated with HRP-conjugated anti-rat or rabbit IgG (simple stain mouse Max Po; Nichirei, Tokyo, Japan) plus 3-amino-9-ethyl carbazole (AEC) substrate for color development (Nichirei). The sections were counterstained with Mayer's hematoxylin (Dako) and images were obtained using an IX50 inverted microscope equipped with a digital imaging system (Olympus, Center Valley, PA). For immunofluorescent analysis, stained sections were incubated with secondary goat anti-rat Ab coupled to Texas Red (Vector Laboratories Inc., Burlingame, CA), rabbit anti-hamster coupled to DyLight 647 (Abcam), or goat anti-rabbit coupled to DyLight 549 (Vector). Cell nuclei were visualized with DAPI (Vector). Slides were mounted with VECTASHIELD (Vector). Fluorescent images were acquired with a laser-scanning confocal microscope (LSM 510; Zeiss, Thronwood, NY), equipped with a 63x/1.4NA oil objective, or by using fluorescence microscope BZ-9000 and BZ-X700 (Keyence, Tokyo, Japan). Data were derived by counting the number of cells in 20 independent images per tumor group and expressed as cells/mm². M1 and M2 macrophages were identified based on their expression of F4/80⁺CD206⁻ and F4/80⁺CD206⁺, respectively.

Apoptosis analysis

Formalin-fixed paraffin-embedded sections were deparaffinized and processed using the ApopTag Peroxidase or the Fluorescence In Situ Apoptosis Detection Kit (EMD Millipore Corporation, Billerica, MA). DNA fragments were labeled with digoxigenin-nucleotide followed by incubation with a peroxidase-conjugated anti-digoxigenin antibody. Positive signals of peroxidase assay were visualized by AEC (Nichirei).

ELISA

Cytokine levels in BAL, serum, and culture supernatants were measured by ELISA as previously described (24). Briefly, paired IL-6 and IL-12-specific mAbs were purchased from BD Pharmingen. Ninety-six-well Immulon H2B plates (Thermo LabSystems, Beverly, MA) were coated with capture cytokine-specific Abs and then blocked with PBS/1% BSA. Samples were added and bound cytokine detected by the addition of biotin-labeled secondary Ab, followed by phosphatase-conjugated avidin and a phosphatase-specific colorimetric substrate. Standard curves were generated using recombinant cytokines purchased from R&D Systems (Minneapolis, MN).

Statistical Analysis

Statistical analyses were performed using MedCalc, version 13.0 (MedCalc Software, Mariakerke, Belgium). Differences in survival were determined using the log rank test of Kaplan-Meier. Differences between groups were assessed using a one-way ANOVA followed by Student-Newman-Keuls post-hoc test. All tests were two-sided; probability values <0.05 were considered significant. All values are expressed as mean ± SE.

Study approval

Breeding and experiments were reviewed and approved by the Institutional Animal Care and Use Committee of the National Cancer Institute in Frederick.

Results

Effect of CpG ODN on the growth of pulmonary tumors

A well established murine model of NSCLC was used to evaluate the anti-tumor activity of locally vs systemically administered CpG ODN. 10^6 Lewis lung cancer (LLC) cells were instilled into the lungs of syngeneic C57BL/6 mice. Consistent with previous reports, these cells proliferated and formed peri-bronchial tumors resembling those present in patients with NSCLC (Supplemental Fig 1) (22;25).

Mice challenged with LLC had a median survival time of 22 days (Fig 1). Systemic (i.p.) delivery of CpG ODN conferred a modest but statistically insignificant survival benefit (HR: 0.55; 95% CI, 0.24–1.26; $p = 0.11$). Median survival time improved to 38 days (HR: 0.28; 95% CI, 0.13–0.59; $p = 0.01$) when 50 μg of CpG ODN was delivered via the intra-tracheal (i.t.) route directly into the lungs (Fig 1). This effect was sequence specific as control ODN had no effect.

While local delivery of CpG ODN was superior to systemic administration, most mice in both treatment groups still succumbed to lung cancer. As free ODN rapidly diffuse from the lungs into the blood stream, we sought to prolong their pulmonary retention by adsorbing the ODN onto polyketal nanoparticles. Such particles have an excellent *in vivo* safety profile and form microparticles 1–5 μm in diameter (appropriate for delivery to the distal alveoli by inhalation) when freeze dried (Supplemental Fig 2A) (19;26). Preliminary studies showed that 30 μg of ODN was adsorbed per mg of polyketal microparticle and that 80% of the ODN was released from the microparticles over 48 hr under physiologic conditions (Supplemental Fig 2B/C).

To determine whether CpG ODN retained their ability to stimulate cells after polyketal adsorption, the response of splenocytes from WT and TLR9 KO mice was compared. WT cells responded to both free and adsorbed CpG ODN by proliferating and secreting IL-6 and IL-12 during culture ($p < 0.05$, Fig 2). Free CpG was more effective immediately after delivery while CpG adsorbed onto microparticles (CpG-MP) was more effective after 3 days in culture, consistent with the release characteristics of ODN from such particles. As seen in Supplemental Fig 2, less than half of the adsorbed ODN was available at the start of culture, with more being released over time. Two findings established the specificity of these responses: i) cells from TLR9 KO mice failed to respond to CpG ODN (free or polyketal adsorbed) and ii) control (non-CpG) ODN adsorbed onto microparticles had no effect on WT or TLR9 KO cells (Fig 2).

The uptake and longevity of CpG instilled into the lungs of mice with LLC tumors was then examined using fluorescein-conjugated ODN. Six hours after intra-tracheal delivery, free ODN was present primarily on the mucosal surface of the bronchial tree (Fig 3A). By 48 hr, little of this material remained in the bronchi or could be found in association with LLC tumors (Fig 3B). CpG-MP was distributed in bronchial and alveolar spaces at 6 hr (Fig 3C). Of interest, this material persisted through 48 hr at which time it had accumulated in tumor nests (Fig 3D). To identify the cells interacting with the CpG-MP, sections were counterstained with phenotype-specific Abs. Results showed that fluorescein-labeled CpG-

MP associated primarily with cells expressing F4/80 (macrophages) and CD205 (DC) within the tumors (Fig 3 E/F).

CpG-MP activates immune cells *in vivo*

CpG-MP or saline was instilled into the lungs of normal mice. BAL fluid collected 2 days later from animals treated with saline contained on average 4×10^4 cells/ml. Cellularity rose by $\approx 25\%$ in mice treated with free CpG ODN (Fig 4A). By comparison, the BAL of mice treated with CpG-MP contained $\approx 15 \times 10^4$ cells/ml ($p < 0.01$, Fig 4A). This increased cellular infiltrate consisted primarily of macrophages and lymphocytes. Consistent with previous studies, free CpG ODN induced a significant increase in pulmonary IL-12 levels, an effect magnified >10 -fold by delivery of CpG-MP (Fig 4B). No such changes occurred in mice treated with control ODN-MP.

CpG-MP improves the survival of mice with lung cancer

Mice were challenged with 10^6 LLC as described above and then treated weekly for one month with CpG-MP starting on day 7. When delivered systemically (the route by which free CpG ODN was ineffective in phase III human trials) (11;12), CpG-MP nearly doubled median survival time (from 22 days to 40 days, HR: 0.37; 95% CI, 0.14–0.95; $p = 0.007$, Fig 5). Far better results were achieved when CpG-MP was instilled directly into the lungs: 82% of mice survived indefinitely (animals were followed for up to 1 year) (HR: 0.054; 95% CI, 0.024–0.12; $p < 0.0001$ vs untreated controls). Moreover, these surviving mice remained tumor free when re-challenged with LLC months after cessation of CpG-MP therapy (Fig 6 legend). Control ODN-MP delivered i.t. had no significant effect on survival (Fig 5). The survival benefit conferred by CpG-MP was not observed in TLR9 KO or Rag1 KO mice (Supplemental Fig 3), consistent with CpG-MP acting through host immune cells that express TLR9.

Effect of CpG-MP on the tumor immune milieu

To clarify the basis of the anti-tumoral immunity elicited by local delivery of CpG-MP, serial sections were taken through the tumor beds and examined using immunohistology. Initial experiments replicated the survival studies described above: mice were treated with CpG-MP 7 and 14 days after LLC instillation and their tumors analyzed on day 20. Consistent with the survival data shown in Fig 5, recipients of CpG-MP had significantly fewer and smaller tumor nodules than control animals with overall tumor burden being reduced by $>90\%$ (Fig 6A). The frequency of apoptotic cells in these tumors rose by ≈ 3 -fold while the number of CD8⁺ T cells infiltrating the tumor site increased nearly 8-fold ($p < 0.01$ for both parameters, Fig 6 B/C and Supplemental Figs 4A/B and 5A).

Several additional changes in immune cell frequency were observed after CpG-MP treatment. Immunohistologic analysis of serial lung sections showed that the frequency of immunosuppressive cells in the tumor microenvironment (Tregs plus M2 macrophages) declined by over half while the number of M1 macrophages doubled ($p < 0.01$, Fig 6D and Supplemental Figs 4C/D and 5B). Thus, the relative frequency of M1:M2 macrophages rose nearly 4-fold in CpG-MP treated animals ($p < 0.01$, Fig 6E).

To gain insight into the relationships between these changes, the kinetics with which they occurred was evaluated by treating mice only once (18 days after LLC instillation) with CpG-MP. Tumors were studied two days later. At that early time point post treatment, increased tumor cell apoptosis was already evident (2-fold, $p < 0.01$, Fig 6B) as was the increase in infiltrating CD8 T cells ($p < 0.01$, Fig 6C and Supplemental Figs 4,5). Concomitantly, the frequency of immunosuppressive Tregs and M2 macrophages decreased significantly ($p = 0.05$, Fig 6D and Supplemental Figs 4,5). However no effect on M1 macrophages or M1:M2 ratio was detected two days after treatment (Fig 6E). Together, these findings suggest that CpG-MP rapidly reduces local immune suppression, enabling the infiltration of tumoricidal CD8 T cells that support tumor cell apoptosis. The magnitude of these effects increases over time and with repeated therapy and is accompanied by a slower rise in the frequency of M1 macrophages ($p < 0.01$, Fig 6E and Supplemental Fig 4).

Discussion

Cells that express TLR9 contribute to tumor-specific host immune responses (27–30). Yet systemic treatment with CpG ODN has been of limited benefit to patients or animals with lung cancer (11–12;31–33). Animal models of melanoma and kidney/colon carcinoma suggest that optimal CpG ODN therapy requires local (rather than systemic) delivery (6;7). Building on that finding we explored the utility of instilling CpG ODN directly into the lungs of mice with LLC tumors (Fig 1). The LLC model shares important features of primary human lung cancer including the peribronchial localization of tumors nodules and the presence of tumor-induced bronchial associated lymphoid tissue (Supplemental Fig 1) (22;23;34;35).

Consistent with previous findings, systemic delivery of CpG ODN had little effect on survival (31). Outcomes improved when the ODN was delivered intratracheally but survival remained modest (Fig 1). Biodistribution studies showed that free ODN i) localized to the mucosal and submucosal regions of the bronchus rather than reaching tumor-associated immune cells and ii) was rapidly cleared from the lungs (Figs 3A and 3B).

To improve the uptake and persistence of ODN in the tumor microenvironment, CpG ODN were adsorbed onto biodegradable polyketal nanoparticles and then freeze dried to form aggregates of optimize size for delivery throughout the bronchial tree (Supplemental Fig 2) (36;37). This differed from earlier efforts in which ODN was simply mixed with 25 – 30 nanometer particles (38;39). CpG ODN adsorbed onto MP retained their sequence specific ability to activate TLR9-expressing cells and were well tolerated (Fig 2). Previous studies established that the small size and positive charge of free ODN resulted in their rapid redistribution through total body fluid. In contrast, CpG-MP remained in the lungs for up to 6 days where they induced an inflammatory response and accumulated within tumor nests after intrapulmonary instillation (Figs 3, 4). Systemic administration of CpG-MP did not achieve this goal (Fig 5), consistent with earlier reports that such particles are primarily trapped and removed from the circulation by the liver (40). Preliminary studies found that 50 μg of CpG ODN delivered weekly for one month provided optimal protection in the LLC challenge model, and effect dependent on the presence of TLR9-expressing immune cells (Fig 5 and Supplemental Fig 3). Lowering the dose of ODN to 10 μg reduced long term

survival from >80 % to <40 % (HR: 0.33; 95% CI, 0.11–1.03; $p = 0.05$ vs No Rx). The immunity induced by CpG ODN therapy was persistent in that no tumors arose when survivors were re-challenged with LLC.

Increased numbers of Foxp3⁺ regulatory T cells are a negative prognostic indicator for patients with lung cancer (41–43). Consistent with that observation, we observed an inverse relationship between the frequency of Tregs and apoptotic cells in LLC tumors (Fig 6, $r = -0.47$, $p = 0.008$). Clinical studies also indicate that patient survival correlates positively with M-1 but inversely with M-2 like macrophage frequency (44–46). This is not unexpected, as M1 macrophages support the inflammation that aids tumor rejection while M2 macrophages facilitate tumor growth by suppressing tumoricidal CTL and NK cells (47). Treatment with CpG-MP altered macrophage abundance, resulting in a 4-fold increase in the frequency of M1:M2 macrophages in the tumor bed (Fig 6E).

Previous reports documented the ability of TLR9 agonists to promote the development of tumoricidal T and NK cells (28;30;48). Current findings establish that these CD8 T cells are better able to reach and lyse pulmonary tumors when the CpG ODN is absorbed onto microparticles and delivered to the lungs (Fig 6C and Supplemental Fig 4A/B). This therapeutic approach achieved 80% long term survival of animals that would otherwise succumb to cancer in 22 days. Mechanistically, local administration of CpG-MP triggered a rapid decline in the number of Tregs and M2-like macrophages within the tumor (Fig 6D and Supplemental Fig 5B) (13;49). This was associated with an influx of CD8 T cells that correlated with increased tumor cell apoptosis (Fig 6 and Supplemental Fig 5A). The magnitude of these effects increased over time and with repeated therapy. As intra-tracheal instillation of LLC generated peribronchial tumors whether equivalent benefit will be observed in the treatment of primary or metastatic tumors in the lung periphery is uncertain. Biodistribution studies show that intra-tracheally administered CpG-MP do reach peripheral tumors but their effectiveness needs to be established in studies of additional lung cancer models. Available data shows that adsorption onto polyketal microparticles enhances the delivery and persistence of immunostimulatory CpG ODN in the lungs, offering hope for substantially improved therapy of pulmonary tumors.

Supplementary Material

Refer to Web version on PubMed Central for supplementary material.

Acknowledgments

Financial support: D.M. Klinman's lab is internally funded by the NCI. T. Sato received grants (Nos. 21790778, 23790917 and 15K09224) from the Ministry of Education, Culture, Sports, Science, and Technology of Japan.

The assertions herein are the private ones of the authors and are not to be construed as official or as reflecting the views of the National Cancer Institute at large.

References

1. Siegel R, Naishadham D, Jemal A. Cancer statistics, 2013. *CA Cancer J Clin.* 2013; 63:11–30. [PubMed: 23335087]

2. Verhoef C, de Wilt JH, Burger JW, Verheul HM, Koopman M. Surgery of the primary in stage IV colorectal cancer with unresectable metastases. *Eur J Cancer*. 2011; (Suppl 3):S61–S66. [PubMed: 21944031]
3. Chang GJ. Challenge of primary tumor management in patients with stage IV colorectal cancer. *J Clin Oncol*. 2012; 30:3165–6. [PubMed: 22869881]
4. Bradbury PA, Shepherd FA. Immunotherapy for lung cancer. *J Thorac Oncol*. 2008; 3(Suppl 2):S164–S170. [PubMed: 18520304]
5. Rakoff-Nahoum S, Medzhitov R. Toll-like receptors and cancer. *Nat Rev Cancer*. 2009; 9:57–63. [PubMed: 19052556]
6. Krieg AM. Development of TLR9 agonists for cancer therapy. *J Clin Invest*. 2007; 117:1184–94. [PubMed: 17476348]
7. Klinman DM. Immunotherapeutic uses of CpG oligodeoxynucleotides. *Nat Rev Immunol*. 2004; 4:249–58. [PubMed: 15057783]
8. Weeratna RD, Bourne LL, Sullivan SM, Davis HL, Krieg A. Combination of a new TLR9 agonist immunomodulator (CpG 7909) and paclitaxel for treatment of metastatic Lewis Lung Carcinoma (LLC). *J Clin Oncol*. 2004; 22:702S.
9. Manegold C, Gravenor D, Woytowicz D, Mezger J, Hirsh V, Albert G, et al. Randomized phase II trial of a toll-like receptor 9 agonist oligodeoxynucleotide, PF-3512676, in combination with first-line taxane plus platinum chemotherapy for advanced-stage non-small-cell lung cancer. *J Clin Oncol*. 2008; 26:3979–86. [PubMed: 18711188]
10. Yamada K, Nakao M, Fukuyama C, Nokihara H, Yamamoto N, Sekine I, et al. Phase I study of TLR9 agonist PF-3512676 in combination with carboplatin and paclitaxel in patients with advanced non-small-cell lung cancer. *Cancer Sci*. 2010; 101:188–95. [PubMed: 19843072]
11. Hirsh V, Paz-Ares L, Boyer M, Rosell R, Middleton G, Eberhardt WE, et al. Randomized phase III trial of paclitaxel/carboplatin with or without PF-3512676 (Toll-like receptor 9 agonist) as first-line treatment for advanced non-small-cell lung cancer. *J Clin Oncol*. 2011; 29:2667–74. [PubMed: 21632509]
12. Manegold C, van ZN, Szczesna A, Zatloukal P, Au JS, Blasinska-Morawiec M, et al. A phase III randomized study of gemcitabine and cisplatin with or without PF-3512676 (TLR9 agonist) as first-line treatment of advanced non-small-cell lung cancer. *Ann Oncol*. 2012; 23:72–7. [PubMed: 21464154]
13. Shirota Y, Shirota H, Klinman DM. Intratumoral injection of CpG oligonucleotides induces the differentiation and reduces the immunosuppressive activity of myeloid-derived suppressor cells. *J Immunol*. 2012; 188:1592–9. [PubMed: 22231700]
14. Tatsumura T, Koyama S, Tsujimoto M, Kitagawa M, Kagamimori S. Further study of nebulisation chemotherapy, a new chemotherapeutic method in the treatment of lung carcinomas: fundamental and clinical. *Br J Cancer*. 1993; 68:1146–9. [PubMed: 8260366]
15. Otterson GA, Villalona-Calero MA, Sharma S, Kris MG, Imondi A, Gerber M, et al. Phase I study of inhaled Doxorubicin for patients with metastatic tumors to the lungs. *Clin Cancer Res*. 2007; 13:1246–52. [PubMed: 17317836]
16. Otterson GA, Villalona-Calero MA, Hicks W, Pan X, Ellerton JA, Gettinger SN, et al. Phase I/II study of inhaled doxorubicin combined with platinum-based therapy for advanced non-small cell lung cancer. *Clin Cancer Res*. 2010; 16:2466–73. [PubMed: 20371682]
17. Arndt CA, Koshkina NV, Inwards CY, Hawkins DS, Krailo MD, Villaluna D, et al. Inhaled granulocyte-macrophage colony stimulating factor for first pulmonary recurrence of osteosarcoma: effects on disease-free survival and immunomodulation. a report from the Children's Oncology Group. *Clin Cancer Res*. 2010; 16:4024–30. [PubMed: 20576718]
18. Heffernan MJ, Murthy N. Polyketal nanoparticles: a new pH-sensitive biodegradable drug delivery vehicle. *Bioconjug Chem*. 2005; 16:1340–2. [PubMed: 16287226]
19. Fiore VF, Lofton MC, Roser-Page S, Yang SC, Roman J, Murthy N, et al. Polyketal microparticles for therapeutic delivery to the lung. *Biomaterials*. 2010; 31:810–7. [PubMed: 19846216]
20. Heffernan MJ, Kasturi SP, Yang SC, Pulendran B, Murthy N. The stimulation of CD8+ T cells by dendritic cells pulsed with polyketal microparticles containing ion-paired protein antigen and poly(inosinic acid)-poly(cytidylic acid). *Biomaterials*. 2009; 30:910–8. [PubMed: 19036430]

21. Tahara K, Sakai T, Yamamoto H, Takeuchi H, Kawashima Y. Establishing chitosan coated PLGA nanosphere platform loaded with wide variety of nucleic acid by complexation with cationic compound for gene delivery. *Int J Pharm.* 2008; 354:210–6. [PubMed: 18178349]
22. Savai R, Wolf JC, Greschus S, Eul BG, Schermuly RT, Hanze J, et al. Analysis of tumor vessel supply in Lewis lung carcinoma in mice by fluorescent microsphere distribution and imaging with micro- and flat-panel computed tomography. *Am J Pathol.* 2005; 167:937–46. [PubMed: 16192630]
23. Savai R, Langheinrich AC, Schermuly RT, Pullamsetti SS, Dumitrascu R, Traupe H, et al. Evaluation of angiogenesis using micro-computed tomography in a xenograft mouse model of lung cancer. *Neoplasia.* 2009; 11:48–56. [PubMed: 19107231]
24. Klinman, DM.; Nutman, TB. ELISpot assay to detect cytokine-secreting murine and human cells. In: Coligan, JE.; Kruisbeek, AM.; Margulies, DH.; Shevach, EM.; Strober, W., editors. *Current Protocols in Immunology.* 7. Brooklyn, NY: Greene Publishing Associates; 1994.
25. Doki Y, Murakami K, Yamaura T, Sugiyama S, Misaki T, Saiki I. Mediastinal lymph node metastasis model by orthotopic intrapulmonary implantation of Lewis lung carcinoma cells in mice. *Br J Cancer.* 1999; 79:1121–6. [PubMed: 10098745]
26. Lee S, Yang SC, Heffernan MJ, Taylor WR, Murthy N. Polyketal microparticles: a new delivery vehicle for superoxide dismutase. *Bioconjug Chem.* 2007; 18:4–7. [PubMed: 17226951]
27. Kawarada Y, Ganss R, Garbi N, Sacher T, Arnold B, Hammerling GJ. NK- and CD8(+) T cell-mediated eradication of established tumors by peritumoral injection of CpG-containing oligodeoxynucleotides. *J Immunol.* 2001; 167:5247–53. [PubMed: 11673539]
28. Heckelsmiller K, Rall K, Beck S, Schlamp A, Seiderer J, Jahrsdorfer B, et al. Peritumoral CpG DNA elicits a coordinated response of CD8 T cells and innate effectors to cure established tumors in a murine colon carcinoma model. *J Immunol.* 2002; 169:3892–9. [PubMed: 12244187]
29. Lonsdorf AS, Kuekrek H, Stern BV, Boehm BO, Lehmann PV, Tary-Lehmann M. Intratumor CpG-oligodeoxynucleotide injection induces protective antitumor T cell immunity. *J Immunol.* 2003; 171:3941–6. [PubMed: 14530311]
30. Baines J, Celis E. Immune-mediated tumor regression induced by CpG-containing oligodeoxynucleotides. *Clin Cancer Res.* 2003; 9:2693–700. [PubMed: 12855649]
31. Sorrentino R, Morello S, Luciano A, Crother TR, Maiolino P, Bonavita E, et al. Plasmacytoid dendritic cells alter the antitumor activity of CpG-oligodeoxynucleotides in a mouse model of lung carcinoma. *J Immunol.* 2010; 185:4641–50. [PubMed: 20855872]
32. Sorrentino R, Morello S, Forte G, Montinaro A, De VG, Luciano A, et al. B cells contribute to the antitumor activity of CpG-oligodeoxynucleotide in a mouse model of metastatic lung carcinoma. *Am J Respir Crit Care Med.* 2011; 183:1369–79. [PubMed: 21278302]
33. Belani CP, Nemunaitis JJ, Chachoua A, Eisenberg PD, Raez LE, Cuevas JD, et al. Phase 2 trial of erlotinib with or without PF-3512676 (CPG 7909, a Toll-like receptor 9 agonist) in patients with advanced recurrent EGFR-positive non-small cell lung cancer. *Cancer Biol Ther.* 2013; 14:557–63. [PubMed: 23792641]
34. Dieu-Nosjean MC, Antoine M, Danel C, Heudes D, Wislez M, Poulot V, et al. Long-term survival for patients with non-small-cell lung cancer with intratumoral lymphoid structures. *J Clin Oncol.* 2008; 26:4410–7. [PubMed: 18802153]
35. Wang HY, Ross HM, Ng B, Burt ME. Establishment of an experimental intrapulmonary tumor nodule model. *Ann Thorac Surg.* 1997; 64:216–9. [PubMed: 9236364]
36. Langer R. Drug delivery and targeting. *Nature.* 1998; 392:5–10. [PubMed: 9579855]
37. Labiris NR, Dolovich MB. Pulmonary drug delivery. Part I: physiological factors affecting therapeutic effectiveness of aerosolized medications. *Br J Clin Pharmacol.* 2003; 56:588–99. [PubMed: 14616418]
38. Ballester M, Nembrini C, Dhar N, de TA, de PC, Pasquier M, et al. Nanoparticle conjugation and pulmonary delivery enhance the protective efficacy of Ag85B and CpG against tuberculosis. *Vaccine.* 2011; 29:6959–66. [PubMed: 21787826]
39. Nembrini C, Stano A, Dane KY, Ballester M, van d V, Marsland BJ, et al. Nanoparticle conjugation of antigen enhances cytotoxic T-cell responses in pulmonary vaccination. *Proc Natl Acad Sci U S A.* 2011; 108:E989–E997. [PubMed: 21969597]

40. Davis ME, Chen ZG, Shin DM. Nanoparticle therapeutics: an emerging treatment modality for cancer. *Nat Rev Drug Discov*. 2008; 7:771–82. [PubMed: 18758474]
41. Petersen RP, Campa MJ, Sperlazza J, Conlon D, Joshi MB, Harpole DH Jr, et al. Tumor infiltrating Foxp3+ regulatory T-cells are associated with recurrence in pathologic stage I NSCLC patients. *Cancer*. 2006; 107:2866–72. [PubMed: 17099880]
42. Shimizu K, Nakata M, Hiram Y, Yukawa T, Maeda A, Tanemoto K. Tumor-infiltrating Foxp3+ regulatory T cells are correlated with cyclooxygenase-2 expression and are associated with recurrence in resected non-small cell lung cancer. *J Thorac Oncol*. 2010; 5:585–90. [PubMed: 20234320]
43. Suzuki K, Kadota K, Sima CS, Nitadori J, Rusch VW, Travis WD, et al. Clinical impact of immune microenvironment in stage I lung adenocarcinoma: tumor interleukin-12 receptor beta2 (IL-12Rbeta2), IL-7R, and stromal FoxP3/CD3 ratio are independent predictors of recurrence. *J Clin Oncol*. 2013; 31:490–8. [PubMed: 23269987]
44. Zeni E, Mazzetti L, Miotto D, Lo CN, Maestrelli P, Querzoli P, et al. Macrophage expression of interleukin-10 is a prognostic factor in nonsmall cell lung cancer. *Eur Respir J*. 2007; 30:627–32. [PubMed: 17537769]
45. Ohri CM, Shikotra A, Green RH, Waller DA, Bradding P. Macrophages within NSCLC tumour islets are predominantly of a cytotoxic M1 phenotype associated with extended survival. *Eur Respir J*. 2009; 33:118–26. [PubMed: 19118225]
46. Ohtaki Y, Ishii G, Nagai K, Ashimine S, Kuwata T, Hishida T, et al. Stromal macrophage expressing CD204 is associated with tumor aggressiveness in lung adenocarcinoma. *J Thorac Oncol*. 2010; 5:1507–15. [PubMed: 20802348]
47. Sica A, Schioppa T, Mantovani A, Allavena P. Tumour-associated macrophages are a distinct M2 polarised population promoting tumour progression: potential targets of anti-cancer therapy. *Eur J Cancer*. 2006; 42:717–27. [PubMed: 16520032]
48. Nierkens S, den Brok MH, Roelofsen T, Wagenaars JA, Figdor CG, Ruers TJ, et al. Route of administration of the TLR9 agonist CpG critically determines the efficacy of cancer immunotherapy in mice. *PLoS One*. 2009; 4:e8368. [PubMed: 20020049]
49. Guiducci C, Vicari AP, Sangaletti S, Trinchieri G, Colombo MP. Redirecting in vivo elicited tumor infiltrating macrophages and dendritic cells towards tumor rejection. *Cancer Res*. 2005; 65:3437–46. [PubMed: 15833879]

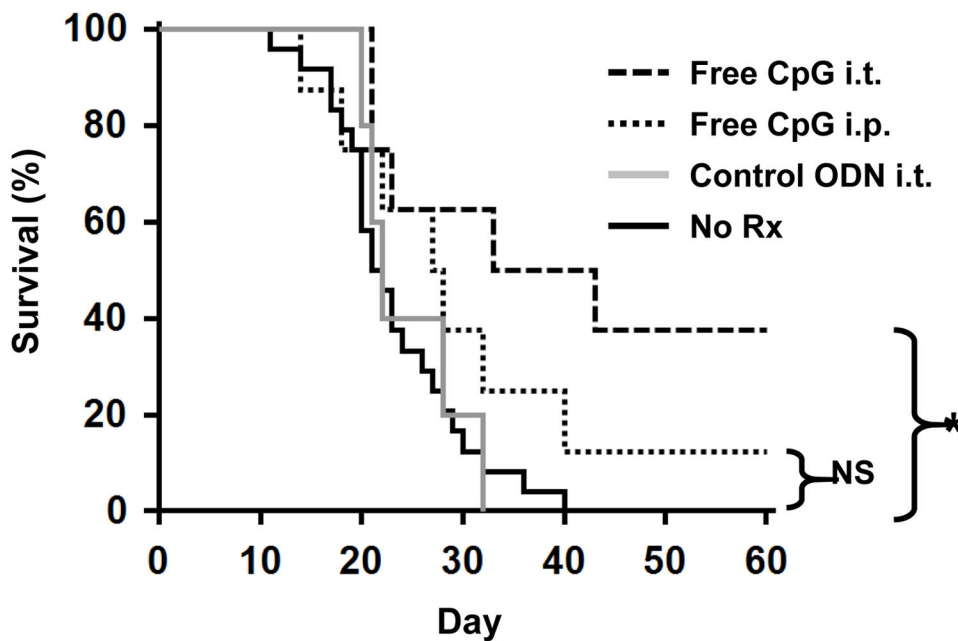


Figure 1. Effect of CpG ODN on survival

10^6 LLC were implanted intra-tracheally into the lungs of syngeneic C57BL/6 mice. Mice were treated with 50 μ g of CpG or control ODN locally (i.t.) or systemically (i.p.) weekly for one month, starting on day 7. Survival was analyzed by Kaplan-Meier statistics using the log-rank test. Data from 2–3 independent experiments involving a total of 5–24 mice/group were combined to generate the survival curves. NS; not significant, *, $p < 0.05$ vs No Rx.

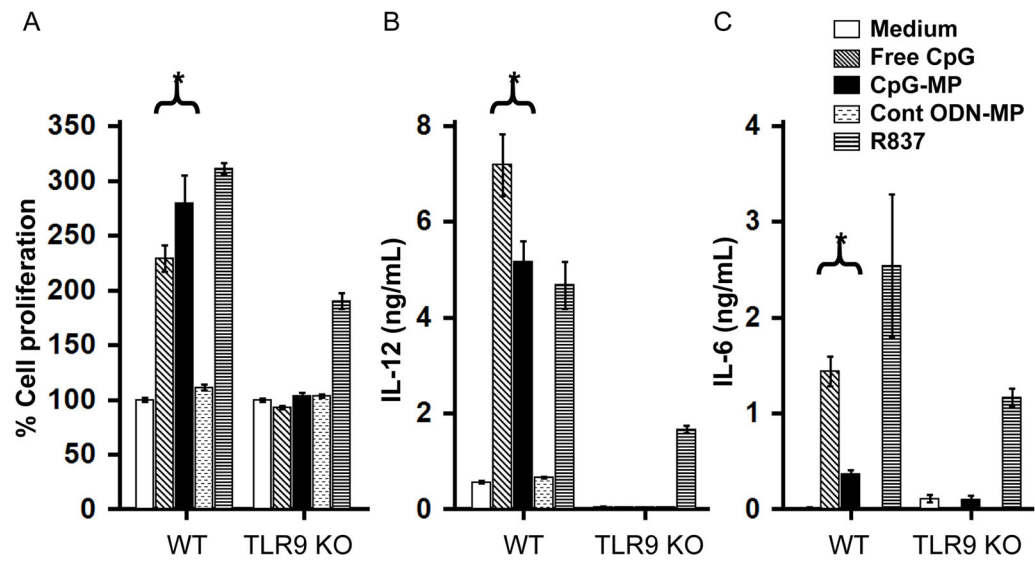


Figure 2. *In vitro* activity of CpG-MP

Spleen cells from WT or TLR9 KO mice were cultured with 1 μ M of free or microparticle (MP) adsorbed CpG ODN or 1 μ g/mL of R837 (TLR7 ligand). A) Cell proliferation after 72 hr. B, C) IL-12 and IL-6 production after 24 hr. Results show the mean \pm SE from 2 independent experiments performed in triplicate. *, $p < 0.05$ (One way Anova).

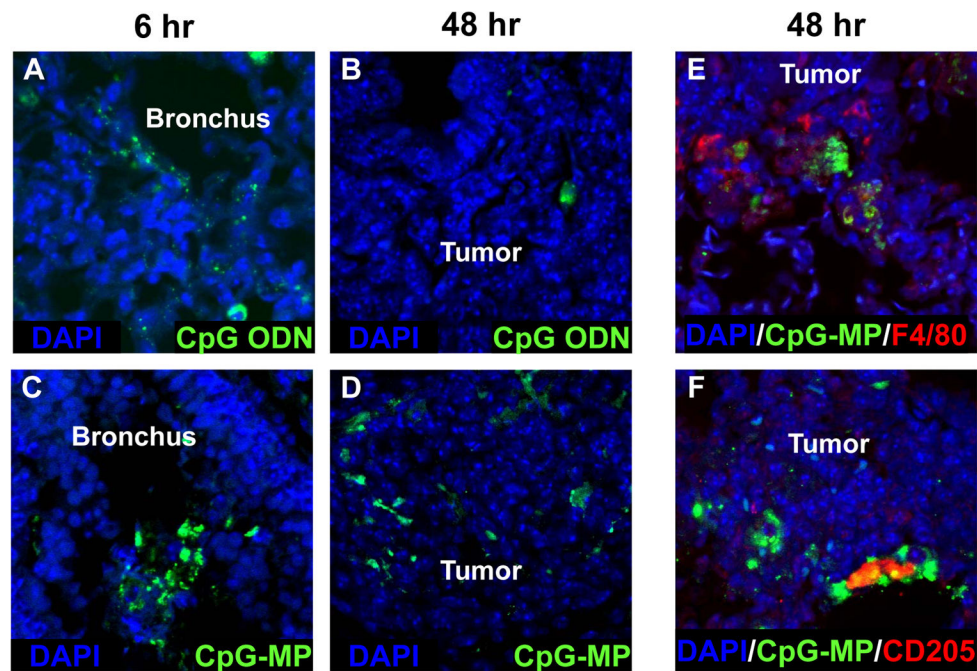


Figure 3. Biodistribution of CpG ODN

LLC were implanted as described in Fig 1. Fluorescein-labeled free CpG ODN (A,B) or CpG-MP (C–F) was delivered i.t. 6 or 48 hr before mice were sacrificed (on day 20). Tissue samples were stained to identify macrophages (red F4/80⁺), DC (red CD205⁺) or CpG (green) and analyzed by confocal microscopy. Note that CpG-MP initially localized to the bronchial mucosa and subsequently accumulated in tumor nests where they remained for up to 6 days.

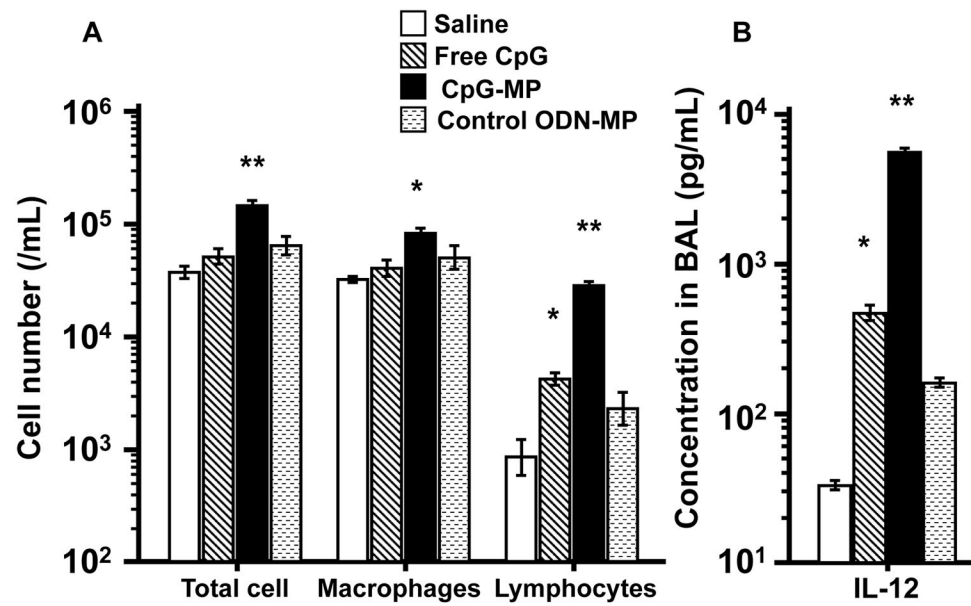


Figure 4. Activity of CpG-MP *in vivo*

50 μ g of CpG ODN (free or adsorbed onto MP) was administered i.t. to normal mice. BAL was collected and analyzed for (A) cellularity and (B) IL-12 levels 2 days later. Results show the mean \pm SE (N = 3–4/group). *, $p < 0.05$, **, $p < 0.01$ vs saline control (One way Anova).

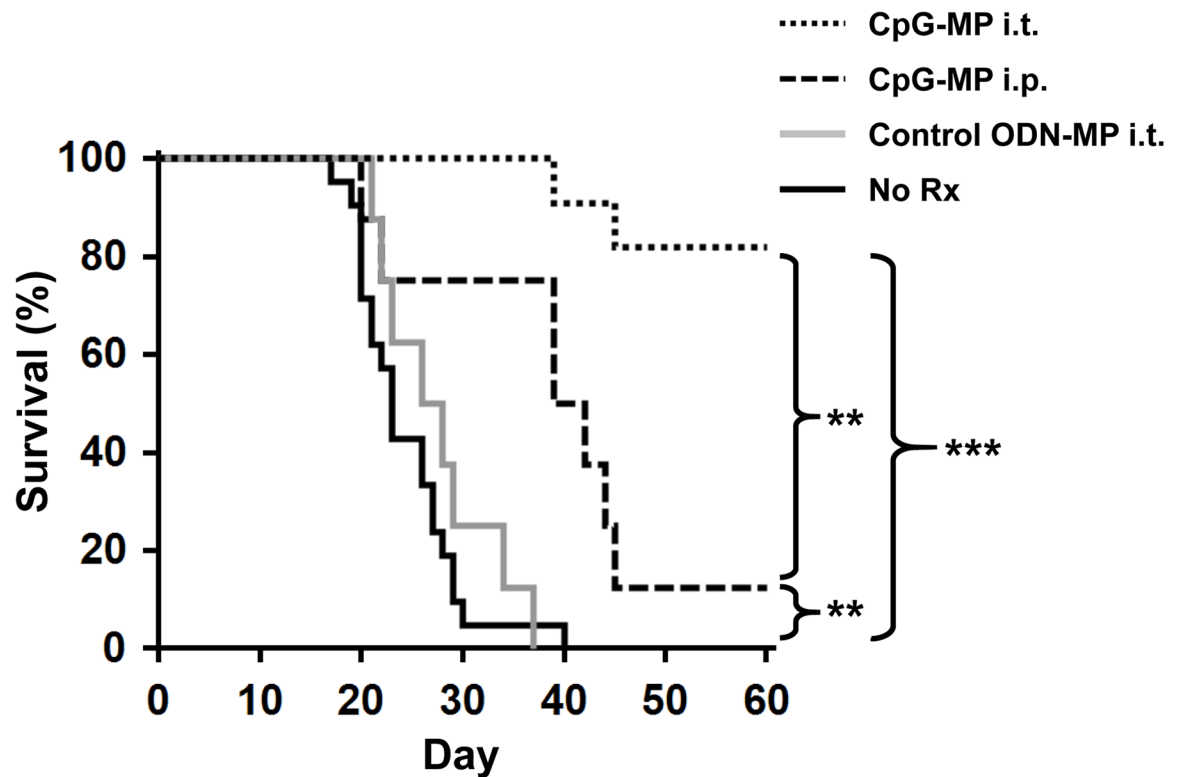


Figure 5. Effect of CpG-MP on survival of LLC challenged mice

LLC were implanted and mice treated with CpG-MP as described in Fig 1. Survival curves were generated and analyzed by Kaplan-Meier statistics using the log-rank test. Data from 3 independent experiments involving 8–21 mice/group were combined to generate each survival curve. Note: surviving mice were re-challenged after 60 days with 5×10^6 LLC. All survived. **, $p < 0.01$, ***, $p < 0.001$ vs No Rx (WT) (Kaplan Meier).

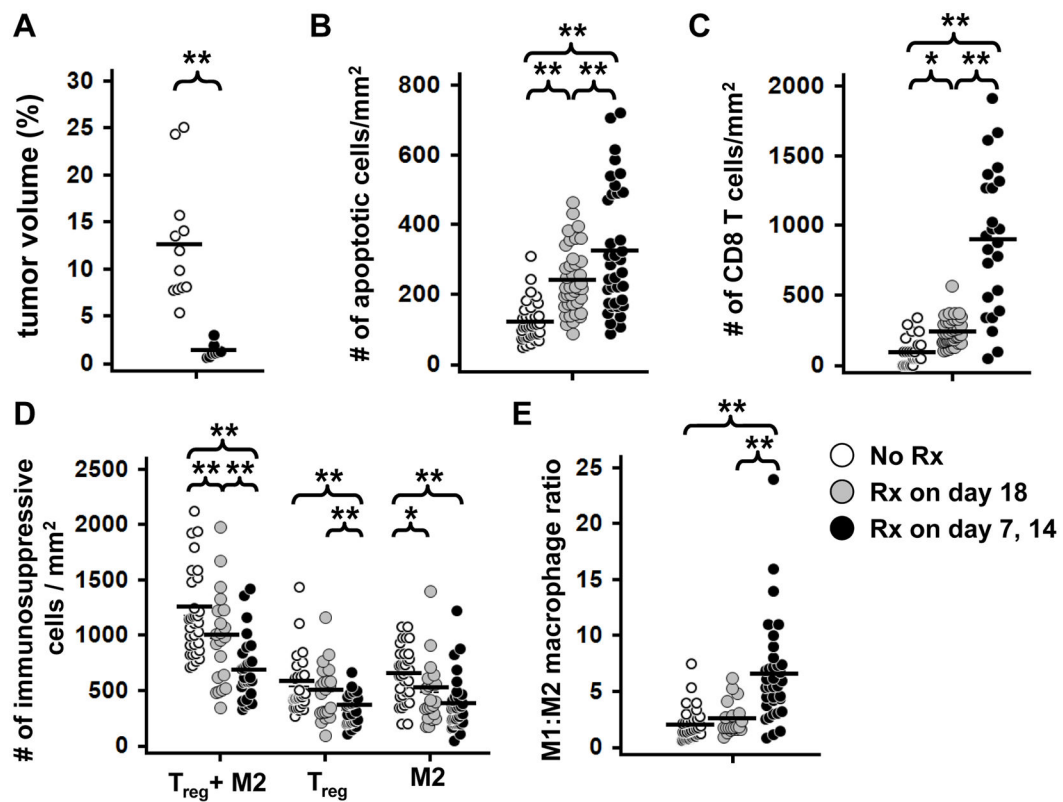


Figure 6. Effect of CpG-MP on tumor infiltrating immune cells

LLC were implanted as described in Fig 1 and mice treated with CpG-MP once on day 18 (gray circles) or twice on days 7 and 14 (black circles). Lungs were collected on day 20. A) Total tumor volume as determined by measuring mid-lung sections from 8–12 mice per group. The total number of (B) apoptotic (TUNEL⁺) cells, (C) CD8⁺ T cells (CD3⁺, CD8⁺), (D) immunosuppressive Treg (Foxp3⁺) plus M2 macrophages (F4/80⁺, CD206⁺) and (E) the ratio of M1 (F4/80⁺ CD206⁻) : M2 macrophages per mm² of tumor was quantified in 15–39 tumors from 3 mice/group. *, $p < 0.05$, **, $p < 0.01$ (One way Anova).